

Systematics of image-state lifetimes on *d* band metal surfaces

H.-S. Rhie,^{1,2} S. Link,¹ H. A. Dürr,^{1,2} W. Eberhardt,^{1,2} and N. V. Smith^{1,3}

¹*Institut für Festkörperforschung, Forschungszentrum Jülich GmbH, 52425 Jülich, Germany*

²*BESSY GmbH, Albert-Einstein-Strasse 15, 12489 Berlin, Germany*

³*Advanced Light Source, Lawrence Berkeley National Laboratory, Berkeley, California 94720, USA*

(Received 24 March 2003; published 30 July 2003)

The fs dynamics of electrons in image states has been modeled on a variety of noble and transition metal surfaces. It is shown that the experimentally observed lifetimes can be described satisfactorily in terms of two key parameters: the penetration length z_0 of the image state into the bulk and the energy phase space S available for the quasiparticle decay.

DOI: 10.1103/PhysRevB.68.033410

PACS number(s): 73.20.-r, 78.47.+p, 79.60.-i

Surface states on metal surfaces represent model systems where electronic excitations in a two-dimensional electron gas coupled to the bulk electronic structure can be studied in detail. Such quasiparticle dynamics is of considerable interest for various physical processes such as chemisorption and desorption at surfaces,¹ femtochemistry,² and magnetization switching.^{3,4} Experimentally one can differentiate between studies of hole and electron quasiparticle dynamics, respectively. Hole lifetimes can be obtained from the quasiparticle linewidths in high resolution photoemission spectroscopy⁵ and scanning tunneling microscopy⁶ experiments. The linewidth contains contributions due to electron-phonon, electron-electron, and electron-defect scattering.⁷ In this paper, however, we focus on electron lifetimes that have been measured directly using pump-probe techniques, and we explore the systematics on varying the surface orientations and going from transition to noble metals.

The dynamics of hot electrons at surfaces can be probed in real time by time-resolved two-photon photoemission spectroscopy. Unoccupied states above the Fermi level E_F are populated with electrons by photoabsorption of fs laser pulses. The transient electron population which is directly related to the lifetime is subsequently probed by time delayed fs laser pulses generating photoelectrons. In particular image states have been systematically studied using this technique (see Table I). Image states are formed when electrons in front of a metal surface are bound by their own image charge induced via electronic screening inside the crystal. When a bandgap prevents the escape into the bulk a series of hydrogeniclike electronic states is formed.⁸ Their binding energy can be reproduced very well by a one-dimensional model potential perpendicular and a nearly free-electron dispersion parallel to the surface.⁸⁻¹⁰ This also provides realistic wavefunctions which are used to evaluate the screened Coulomb interaction responsible for the decay of image states.⁹ In general there is good agreement with first principles calculations that incorporate electron correlation effects to describe the decay processes.⁹ So far these comparisons have been made on a case-by-case basis neglecting the influence of *d* valence electrons.¹² What has been lacking is an intuitive model that extracts the essential physics controlling the systematics of image state lifetimes.

In this paper we describe image state lifetimes by modeling the underlying inelastic scattering processes with two

basic parameters. Scattering matrix elements are approximated by a parameter z_0 describing the wave function overlap of surface and bulk states. The second parameter is the energy phase space S available for quasiparticle decay. It is modeled by a three-way self-convolution of the bulk density of states.^{4,20} With these parameters it appears possible to account for the systematics of all known image state lifetimes on noble and transition metal surfaces.

Transition rates due to electron scattering can be calculated using Fermi's golden rule in the random \mathbf{k} approximation.²¹ This is justified by the strong electron-electron interaction in noble and transition metals which leads to a fast redistribution of electron wave vectors \mathbf{k} . The information about the initial \mathbf{k} values of image state electrons is quickly lost and we can incoherently average over the whole Brillouin zone considering only the energy ϵ exchanged in the inelastic scattering process.⁴ An electron populating an image state with energy E is scattered into a previously unoccupied state with energy $E - \epsilon$. Simultaneously another electron is excited from an energy E' below E_F into a state with energy $E' + \epsilon$ above E_F . The transition rate, i.e., the inverse lifetime, for image state electrons is then given by

TABLE I. Lifetime τ , penetration length z_0 , and phase space parameter S , for the lowest energy image states on face centered cubic metal surfaces discussed in the text.

Surface	τ (fs)	z_0 (Å)	S (10^2 eV ⁻¹)	Ref.
Cu(100)	40 ± 6	5.08	13.9	13
theory	30			9
Cu(111)	18 ± 5	23.9	14.0	15
theory	17.5			9
Ag(100)	55 ± 5	6.72	8.6	13
theory	26.5			14
Ag(111)	30 ± 6	21.2	7.6	16
theory	6			14
Pd(111)	25 ± 4	4.68	76.4	17
theory	22			17
Pt(111)	26 ± 7	8.55	70.5	11,12
theory	29			12
Ni(100)	16 ± 5	4.50	155.9	19
Ni(111)	13 ± 5	5.17	155.3	18

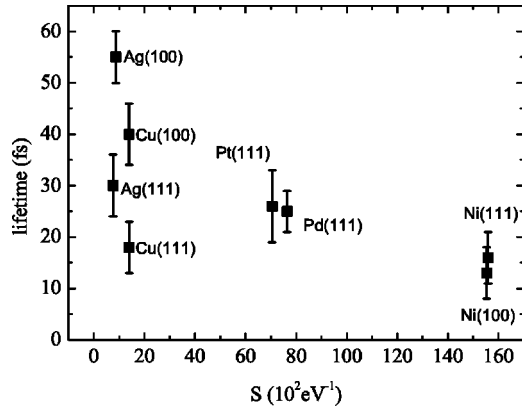


FIG. 1. Lifetimes τ of lowest energy image state electrons plotted against S . The lifetime values are taken from references cited in Table I.

$$1/\tau = (2\pi/\hbar)M^2S, \quad (1)$$

where

$$S = \int_{E_F=0}^E d\epsilon \int_{-\epsilon}^0 dE' \rho(E-\epsilon)\rho(E')\rho(E'+\epsilon) \quad (2)$$

describes the phase space available for the inelastic scattering processes.²⁰ $\rho(E)$ is the total density of electronic states at energy E . The phase space factor S can easily be calculated using tabulated bandstructures of the elemental solids.²² The obtained values of S are included in Table I. Following Ref. 4 we will not differentiate between s, p , or d electrons. We assume constant transition matrix elements, M , for all elements considered. The random \mathbf{k} approximation employed here generally neglects any surface dependence of S . However, we find small variations of S due to the slightly different image state binding energy, e.g., on (100) compared to (111) faces (see Table I).

In Fig. 1 the experimentally measured lowest energy image state lifetimes are plotted against the calculated values of S . The figure shows that the values of S decrease dramatically from Ni to Ag. This is a consequence of the filling up of d bands. However, no scaling according to Eq. (1) is apparent. It is, therefore, necessary to model also the matrix elements. This is done by including a measure of the wave function overlap between image states and the bulk. Since the image state wave function enters M linearly⁴ we can assume $M^2 \propto z_0$. z_0 is the exponential decay length of the image state wave function inside the crystal. It can be calculated using the so-called two-band nearly free electron model.^{8–10} The resulting bandstructure is depicted schematically in the inset of Fig. 2. Inside the bandgap surface state wave functions decay exponentially into the crystal. The decay length z_0 is given by the imaginary part of the complex wave vector component k perpendicular to the surface, $\text{Im}(k) = 1/z_0$, as¹⁰

$$z_0 = d[(4E_g E/V^2 + 1)^{1/2} - (E_g + E)/V]^{-1/2} \quad (3)$$

with $d = [2mV/\hbar^2]^{-1/2}$. Here E is the energy position of the image state, m the effective electron mass, $2V$ the size of the

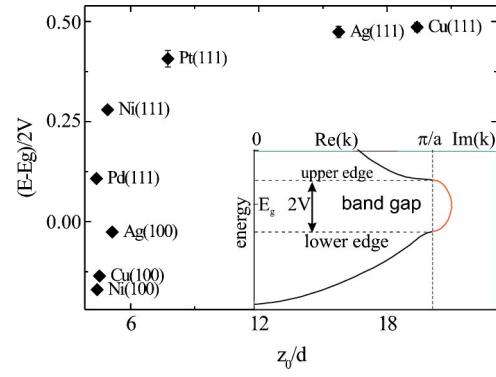


FIG. 2. Energy positions of lowest energy image states relative to the midgap position $E - E_g$ and normalized to the bandgap size $2V$ plotted vs the wave function penetration length z_0 obtained from Eq. (3) for the surfaces in Table I. The inset shows schematically the complex surface band structure.

band gap, and E_g the energy at the zone boundary or simply the energy at the middle of the band gap. All energy positions are referenced to the bottom of the nearly free-electron band which spans the bandgap. From Eq. (3) we calculated z_0 for the metal surfaces listed in Table I. The values for $2V$ and E_g are obtained from data of the upper and lower band gap edges given in Refs. 23–26. Experimental values of E are reported in Refs. 15, 27–29. In Fig. 2 the relative positions of image states inside the bandgap, $(E - E_g)/(2V)$ are shown as a function of the calculated values of z_0/d . It is clearly discernible that at the edges of the bandgap the estimated penetration length is much larger than for states located closer to the bandgap center.

According to Eq. (1) our heuristic model for the lifetime τ should be $1/\tau \propto z_0 S$, i.e., the image state decay rate should increase if the wave function extends deeper into the crystal and if the phase space volume available for scattering is larger. As a corroboration we show in Fig. 3 the experimental values of τ as a function of $z_0 S$. The solid line is a fit of

$$1/\tau = f_{\text{surface}} + f_{\text{bulk}} z_0 S \quad (4)$$

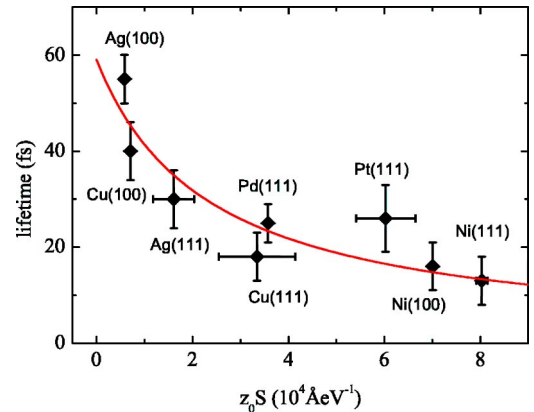


FIG. 3. Lifetimes τ of lowest energy image state electrons plotted against $z_0 S$. The lifetime values are taken from references cited in Table I. The solid line is a least square fit of Eq. (4) to the data.

to the data. We obtain $f_{\text{bulk}} = (7.2 \pm 1.9) \times 10^{-7} \text{ eV fs}^{-1} \text{ \AA}^{-1}$ and $f_{\text{surface}} = (1.7 \pm 0.3) \times 10^{-2} \text{ fs}^{-1}$. The parameter f_{bulk} contains residual matrix elements for the decay into bulk states. In order to obtain a satisfactory fit to the data it is also necessary to include a constant decay rate f_{surface} . This second parameter describes the inelastic scattering of image state electrons into other surface states. Since both types of surface states are localized at similar interface regions this parameter does not depend on the wavefunction penetration into the bulk and on the phase space factor. Image states are known to penetrate less into the bulk with increasing quantum number of the hydrogenic series. This is due to the fact that they are energetically close to the upper edge of the potential barrier on the vacuum side and thus are located further away from the metal surface than the $n=1$ state. This leads to different values of z_0 for different n . Moreover, image states with higher quantum numbers also decay via the lower energy image states.³⁰ Consideration of both effects are beyond the scope of the present paper.

The main result of this paper is that the empirical model described by Eq. (4) reproduces very well the lifetimes of lowest energy image states measured on very different surfaces. This gives us confidence that we have correctly captured the essential physics of image state lifetimes. Some residual scatter of the experimental data around the predicted values might still be discernible in Fig. 3. This could be due to features such as plasmon enhanced decay mechanism that were reported for Ag surfaces.³¹ It has also been pointed out that other surface states contribute differently to f_{surface} on different surfaces even of the same material.⁹ It is also likely that the basic assumption of constant transition matrix elements for different materials is not strictly valid.⁴ Finally we also neglected quantum mechanical interference between bulk and surface decay channels that might play a role.⁹ We note, however, that the resulting deviations from our model are not significant compared to the experimental uncertainties of present day measurements.

Modifying the electronic surface structure by adsorption often dramatically changes the density of states near E_F and can, thus, influence the image state lifetimes. This emphasizes the crucial role of sample preparation which might be responsible for short lifetimes reported in early studies on silver surfaces³² compared to the most recent values compiled in Table I. Concentrating on studies where the surface electronic structure was systematically modified by adsorption we can discuss the observed changes in image state lifetimes^{12,19} within our model. Upon hydrogen adsorption the lifetime of the lowest energy image state on Ni(111) was found to increase by 30%.¹⁹ This was assigned to the quenching of an occupied Ni(111) surface state which decreases the number of decay channels. These effects can be incorporated qualitatively into our model through the f_{surface} parameter. We find that the surface contributes 29% to the total decay rate for Ni(111). If we assume that this surface contribution is quenched by hydrogen adsorption the experimental result is to a large extent reproduced. For oxygen adsorption on Pt(111) a reduction of the image state lifetime larger than 30% was observed and attributed to an increase of the density of states near E_F .¹² This indicates an increase of the decay rate related to bandstructure changes at the surface. If we, for instance, double the surface decay rate f_{surface} for Pt(111) obtained from Fig. 3 we can reproduce the experimental observation.

In conclusion we have presented a model describing the systematics of measured lifetimes of lowest energy image state electrons on noble and transition metal surfaces. The model uses the image state wavefunction penetration, z_0 , into the crystal and the phase space volume S available for inelastic electron scattering as input. Both quantities are evaluated using band energies and density of states taken from reliable band calculations. The lifetimes are calculated by adjusting two free parameters which describe the decay rate into bulk and surface states, respectively. This reproduces all experimentally available lifetime values within their experimental uncertainty.

¹M. Bonn, S. Funk, C. Hess, D.N. Denzler, C. Stampfl, M. Scheffler, M. Wolf, and G. Ertl, *Science* **285**, 5430 (1999).

²A.H. Zewail, *Femtochemistry-Ultrafast Dynamics of the Chemical Bond* (World Scientific, Singapore, 1994).

³E. Beaupaire, J.-C. Merle, A. Daunois, and J.-Y. Bigot, *Phys. Rev. Lett.* **76**, 4250 (1996).

⁴R. Knorren, K.H. Bennenmann, R. Burgermeister, and M. Aeschlimann, *Phys. Rev. B* **61**, 9427 (2000).

⁵F. Reinert, G. Nicolay, S. Schmidt, D. Ehm, and S. Hüfner, *Phys. Rev. B* **63**, 115415 (2001).

⁶J. Klier, R. Berndt, E.V. Chulkov, V.M. Silkin, P.M. Echenique, and S. Crampin, *Science* **288**, 1399 (2000).

⁷A. Eiguen, B. Hellsing, F. Reinert, G. Nicolay, E.V. Chulkov, V.M. Silkin, S. Hüfner, and P.M. Echenique, *Phys. Rev. Lett.* **88**, 066805 (2002).

⁸P.M. Echenique, F. Flores, and F. Sols, *Phys. Rev. Lett.* **55**, 2348 (1985).

⁹E.V. Chulkov, I. Sarria, V.M. Silkin, J.M. Pitarke, and P.M. Echenique, *Phys. Rev. Lett.* **80**, 4947 (1998).

¹⁰N.V. Smith, *Phys. Rev. B* **32**, 3549 (1985).

¹¹S. Link, H.A. Dürr, and W. Eberhardt, *Appl. Phys. A: Mater. Sci. Process.* **71**, 525 (2000).

¹²S. Link, H.A. Dürr, G. Bihlmayer, S. Blügel, W. Eberhardt, E.V. Chulkov, V.M. Silkin, and P.M. Echenique, *Phys. Rev. B* **63**, 115420 (2001).

¹³I.L. Shumay, U. Höfer, Ch. Reu, U. Thomann, W. Wallauer, and Th. Fauster, *Phys. Rev. B* **58**, 13 974 (1998).

¹⁴E.V. Chulkov, V.M. Silkin, and P.M. Echenique, *Surf. Sci.* **391**, L1217 (1997).

¹⁵M. Wolf, E. Knoesel, and T. Hertel, *Phys. Rev. B* **54**, R5295 (1996).

¹⁶J.D. McNeill, R.L. Lingle, Jr., N.-H. Ge, C.M. Wong, R.E. Jordan, and C.B. Harris, *Phys. Rev. Lett.* **79**, 4645 (1997).

¹⁷A. Schäfer, I.L. Shumay, M. Wiets, M. Weinelt, Th. Fauster, E.V. Chulkov, V.M. Silkin, and P.M. Echenique, *Phys. Rev. B* **61**, 13 159 (2000).

- ¹⁸S. Link, J. Sievers, H.A. Dürr, and W. Eberhardt, J. Electron Spectrosc. Relat. Phenom. **114**, 351 (2001).
- ¹⁹S. Link, Ph. D. thesis, Forschungszentrum Jülich, 2001.
- ²⁰C.N. Berglund and W.E. Spicer, Phys. Rev. A **136**, 1030 (1964).
- ²¹D.R. Penn, S.P. Apell, and S.M. Girvin, Phys. Rev. B **32**, 7753 (1985).
- ²²D. A. Papaconstantopoulos, *Handbook of the Band Structure of Elemental Solids* (Plenum, New York, 1986).
- ²³E. Knoesel, A. Hotzel, and M. Wolf, J. Electron Spectrosc. Relat. Phenom. **88–91**, 577 (1998).
- ²⁴N.V. Smith, C.T. Chen, and M. Weinert, Phys. Rev. B **40**, 7565 (1989).
- ²⁵E.V. Chulkov, V.M. Silkin, and P.M. Echenique, Surf. Sci. **437**, 330 (1999).
- ²⁶G. Leschik, R. Courths, H. Wern, S. Hüfner, H. Eckardt, and J. Noffke, Solid State Commun. **52**, 221 (1984).
- ²⁷R. Fischer, S. Schuppler, N. Fischer, Th. Fauster, and W. Steinmann, Phys. Rev. Lett. **70**, 654 (1993).
- ²⁸D.F. Padowith, W.R. Merry, R.E. Jordan, and C.B. Harris, Phys. Rev. Lett. **69**, 3583 (1992).
- ²⁹K. Giesen, F. Hage, F.J. Himpsel, H.J. Riess, and W. Steinmann, Phys. Rev. B **35**, 971 (1987).
- ³⁰I. Sarria, J. Osma, E.V. Chulkov, J.M. Pitarke, and E.P. Echenique, Phys. Rev. B **60**, 11 795 (1999).
- ³¹A. Garcia-Lekue, J.M. Pitarke, E.V. Chulkov, A. Liebsch, and P.M. Echenique, Phys. Rev. Lett. **89**, 096401 (2002).
- ³²R.W. Schoenlein, J.G. Fujimoto, G.L. Eesley, and T.W. Capehart, Phys. Rev. Lett. **61**, 2596 (1988); R.W. Schoenlein, J.G. Fujimoto, G.L. Eesley, and T.W. Capehart, Phys. Rev. B **43**, 4688 (1991).